Research Article

SOHAG JOURNAL OF SCIENCES

https://doi.org/10.21608/sjsci.2024.310920.1218

Study of Structural, Electrical, and Dielectric Properties of Sm-doped $SrMnO_3$

Mahrous R. Ahmed*, H. M. Ali, Amira Etman, E. M. M. Ibrahim, and A. M. Abdel Hakeem

Physics Department, Faculty of Science, Sohag University, Sohag, 82524, Egypt.

**Email: mahrous.r.ahmed@science.sohag.edu.eg*

Received: 20th July 2024, **Revised:** 24th August 2024, **Accepted:** 29th August 2024
Published online: 15th September 2024

Abstract: Structural, morphological, electrical, and dielectric properties of the compound $Sm_xSr_{1-x}MnO_3$, prepared by solid-state reaction and annealed at 650ºC for 8 hours, were investigated. X-ray diffraction results showed that the sample has a monoclinic structure with a $Sm_{0.025}Sr_{0.975}MnO_3$ phase. SEM results showed plate-like perovskite grains which were clustered together in 150 nm grains size. The electrical conductivity which was measured by surface-surface contact showed a semiconductor behavior with increasing the ambient temperature. SEM results reflected that there is less orientation and less connectivity of the grains which confirmed the high resistance of the $Sm_{0.025}Sr_{0.975}MnO_3$ sample at room temperature. The sample had two activation energies; 0.791 eV and 0.761 eV. The Impedance, Z(Ω), AC conductivity, $\sigma_{AC}(\Omega.m)^{-1}$, relative permittivity, ε, and the tangent loss, tan(δ), were investigated for the $Sm_{0.025}Sr_{0.975}MnO_3$ sample. The decrease in sample impedance added to it is used as a dielectric material in the capacitors industry. The AC conductivity had no DC component which depends only on the applied AC only. The decrease of the dielectric constant of the compound was interpreted as the space charge carriers lag after the applied AC field.
Keywords: $Sm_{0.025}Sr_{0.975}MnO_3$, X-ray, SEM, Activation energy, dielectric constant, dielectric loss.

1. Introduction

Manganites, a class of transition metal oxides primarily composed of manganese ions, have emerged as fascinating materials with a diverse array of electronic, magnetic, and structural properties [1, 2]. These compounds, typically characterized by the perovskite crystal structure, have garnered significant scientific interest due to their unique behaviors and potential technological applications across various fields [3].

At the heart of manganites lies the intriguing interplay between charge carriers, spin moment, and lattice phonons, leading to an excess of fascinating phenomena. One of the most notable features of manganites is their colossal magnetoresistance (CMR) effect [4, 5], first discovered in the early 1990s, wherein with applying magnetic field, the dc resistance undergoes a dramatic change [6, 7]. This phenomenon has sparked intense research interest and holds immense promise for applications in spintronics, magnetic sensors, and magnetic storage devices [8, 9].

Moreover, manganites exhibit a phase diagram which is very rich with various magnetic and electronic states, including ferromagnetic, antiferromagnetic, charge-ordered [10, 11], and orbital-ordered [12] phases. The complex phase behavior arises from intricate interactions between charge carriers, magnetic moments, and lattice distortions [13, 14], offering fertile ground for exploring emergent properties and novel functionalities.

Among the numerous of manganite compounds, lanthanum manganite, LaMnO3 [15] which stands out as a prototypical example, extensively studied for its CMR behavior and diverse phase transitions. Other members of the manganite family, such as yttrium manganite, $YMnO_3$, [16] and strontium manganite, $SrMnO_3$, [17-23] which exhibit exciting properties that have attracted considerable attention from researchers.

Unique physical properties with an intense manifestation of interactions between the electron, phonon and magnetic subsystems were exhibited in the $Sm_xSr1\text{-}_xMnO_3$ manganites due to the large difference between the ionic radii of samarium and strontium [24].

There is a gap between our work and previous work such that according to our search about this compound it was found that most of previous published papers about that compound did not used the solid state reaction in preparing the compound under the conditions used in our manuscript.

Besides, despite significant progress in understanding manganite physics, many fundamental questions remain unanswered, particularly regarding the microscopic mechanisms underlying their exotic behaviors. Ongoing research efforts aim to unravel the underlying physics, explore new applications and functionalities, and realize the full potential of manganites in various technological applications for $Sm_xSr_{1-x}MnO_3$ with x=0.025.

2. Synthesization and measurements methods

The experimental techniques used in our work were presented in ref. [24]. The initial step was to use SrO, MnO_3 to make the main compound, $SrMnO_3$, and then dope it with SmO according to the $Sm_xSr_{1-x}MnO_3$ formula, here in the current work x=0.025. In the second step, the sample was ground well for 12 hours to make sure all the compounds were mixed. Then, it was compressed to obtain tablets using the cold

pressing technique. Afterward, in order to improve the homogeneity between the mixtures (SrO, SmO, MnO_3), a heat furnace was used for 8 hours at 650 °C, then, the samples was grounded for 3 hrs to give a sample in ground powder shape with grains size in nano sacle. This process is called solid-state reaction method.

The interplanar spacing (d), crystal structure phases of our powder samples were investigated using X-ray diffraction model ((Philips X'pert MRD) with Cu-Ka radiation (i.e., λ = 1.5418 A), and with angles range of scan from 10° to 100°.

Scanning Electron Microscopy (SEM) (a JSM-6100 microscope (JEOL, Japan) with an acceleration voltage of 30KV, magnification ranging from 14 to 1000000, and resolution for gun 1n, was used to test the surface morphology and compositional subjects of the powder sample.

The resistance of $Sm_xSr_{1-x}MnO_3$ bulk on glass was measured in air using the surface-surface contact method. Temperature range: 303-573 K. An aluminum block served as a sample holder-cum-heater. The sample's resistance and temperature were measured using an ohmmeter (UT71E-TRUE RMS MULTIMETERS) and a chromel-alumel thermocouple in close contact with the surface.

The dielectric constant (ε'), the dielectric loss factor (ε''), impedance (Z), and the AC conductivity (σ_{ac}) were determined by using IM 3536 LCR Meter HIOKI in the frequencies range of 10 – 10^6 Hz.

3. Results and Discussion

3.1. Samples analysis

3.1.1. X-ray diffraction

The structure, crystallinity, and phase purity of $Sm_xSr_{1-x}MnO_3$ with (x= 0.025) are investigated by X-Ray diffraction device. The XRD scan is done with an initial 2θ = 10 degree, final 2θ = 100 and step width = 0.025 degree. Fig. 1 shows the XRD pattern of the sample owning the ratio x = 0.025. The sharp reflection peaks from the crystallographic planes are coinciding with the file COD.1006169 having a single phase; monoclinic phase [25, 26].

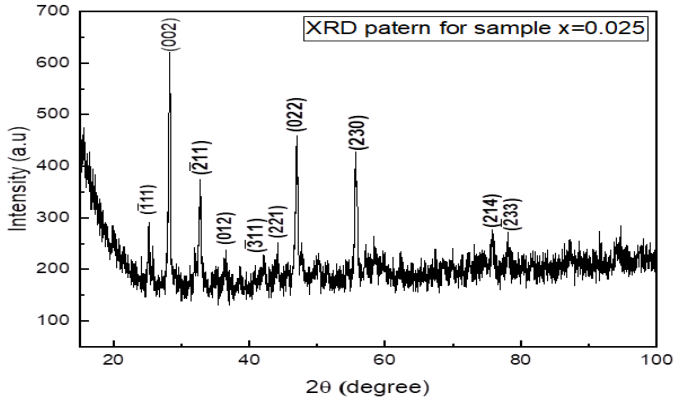

Figure 1: XRD pattern for $Sm_xSr_{1-x}MnO_3$ with (x= 0.025).

Lattice parameters are calculated to ensure the monoclinic structure, the following equations is used:

$$1/d^2 = h^2 / (a^2 \sin^2 \beta) + k^2 / b^2 + l^2 / (c^2 \sin^2 \beta) - 2\, hl \cos\beta/(ac \sin^2 \beta) \quad (1)$$

$$V=abc\ (\sin\beta) \quad (2)$$

Equation (1) states the relation between lattice parameters and d-spacing and equation (2) is used for unit cell volume calculation.

Table 1: The calculated lattice parameters for $Sm_{0.025}Sr_{0.975}\ MnO_3$ sample.

Position (2θ)	(hkl)	FWHM (degree)	d-spacing (A°)
25.1884	(-111)	0.1535	3.53569
28.3231	(002)	0.2047	3.15110
32.7549	(-211)	0.1791	2.73417
36.4349	(012)	0.6140	2.46602
42.1283	(-311)	0.6140	2.14499
44.1213	(221)	0.4093	2.05261
47.0044	(022)	0.1791	1.93322
50.0574	(230)	0.6410	1.82223
55.6609	(214)	0.2558	1.65133
75.7998	(233)	0.3070	1.25502

Crystallite size is obtained by the Scherer equation as follows:

$$D = \frac{k\lambda}{\beta \cos(\theta)} \quad (3)$$

where β is the Full Width at Half Maximum (FWHM), θ the diffraction angle, k is a geometrical factor depending on the diffractometer properties, k= 0.95, and λ is the wavelength of K_α Cu source, λ = 1.5406 (Å). All these parameters are listed in table (1). The value of the crystallite size according to the Scherer equation is obtained from the major peak; D = 105.8672 nm.

The lattice parameters, a, b and c, the lattice angles, α and the unit cell volume, $V(A^o)^3$, for our compound, are tabulated in Table 2.

Table 2: The lattice parameters, the crystalline size of the sample $Sm_{0.025}Sr_{0.975}\ MnO_3$

a (Å)	b (Å)	c (Å)	α (degree)	β (degree)	γ (degree)	V $(Å)^3$
7.65280	5.48904	5.49834	90	90.825	90	64.09

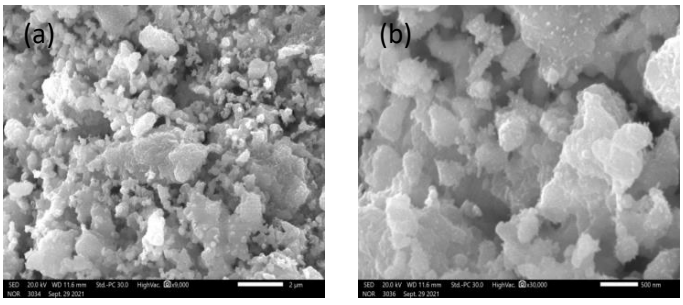

Figure 2: Morphology images magnified by (a) 9000 times, and (b) 30000 times, of the $Sm_{0.025}Sr_{0.975}MnO_3$ sample.

3.1.2. Morphological study

The surface morphology of $Sm_{0.025}Sr_{0.975}MnO_3$ sample is investigated using the Scanning Electron Microscopy (SEM)

technique as shown in Fig. 2. The SEM photomicrograph shows plate-like perovskite grains which are clustered together. It reflects that there is less oriented and less connected grains. This confirms the high resistance of the $Sm_{0.025}Sr_{0.975}MnO_3$ sample at room temperature in the electrical measurements (semiconductor behavior). The size of particles is calculated by imageJ program as depicted in Fig. 3. 150 nm is the calculated average particle size of the perovskite sample.

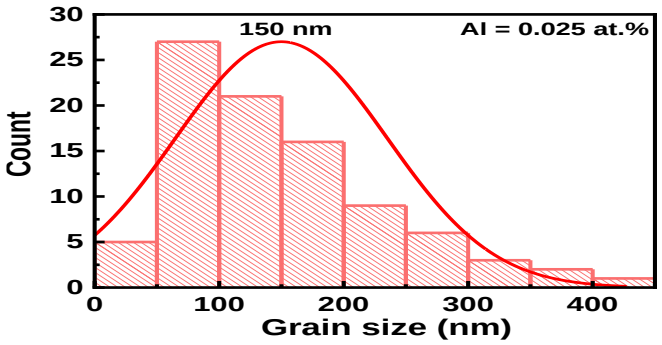

Figure 3: The histogram of the particle size distribution determined from SEM images of the $Sm_{0.025}Sr_{0.975}MnO_3$ sample.

It is noticed from Fig. 3 that the avarege grains sized extracted from SEM images, 150 nm, of the $Sm_{0.025}Sr_{0.975}MnO_3$ sample is higher than that calculated from the XRD results indicating that particle may consist of many grains.

3.2. Electrical properties

In this section the electrical study is implemented in order to check out the electrical behavior of the compound $Sm_{0.025}Sr_{0.975}MnO_3$ sample and its activation energy.

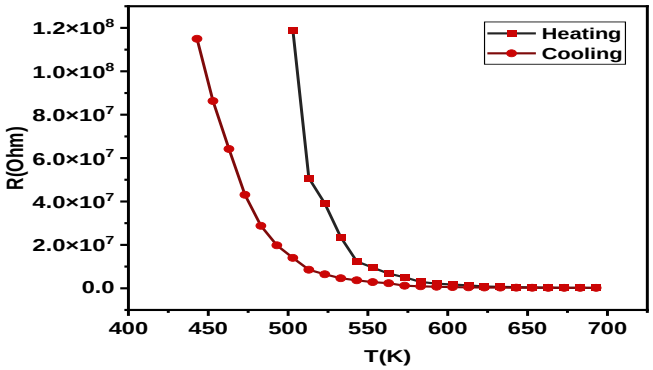

Figure 4: The depencence of the sample resistance, R(Ω), on the ambient temperature, T(K), at increasing and decreasing of temperature for $Sm_{0.025}Sr_{0.975}MnO_3$ sample.

Figure 4 shows the sample resistance, R(Ω),dependence on the ambient temperature, T(K) during the heating and cooling. It is seen from the figure that R(Ω) decreases quickly with the increase of the temperature in small range of T(K); from 450K to 550 k, then, it is nearly stable at the high range of temperature. The resistance behavior of the sample is consistent with that of the semiconductors where the resistant values are about 10^8 Ω . There is a big deviation between $R_{heating}$ and $T_{cooling}$ through the low values of T. It is noticed that the doping process of Sm encourages a lowering in the energy of the activation obtained from a decrease in energy barriers to the polaron's motion. Hence, the doping process in Sm raises the delocalization of charge carriers, and sequentially decreases the resistant [27]. The cductivity in the insulator at the low temperature range is presented because of the electron–phonon interaction and electron–electron interaction respectively according to the suggestion of 2D VRH and 3D VRH models [28]. Also, perovskite grains are clustered together as shown from SEM results which reflecting the less oriented and less connected grains. This confirms the high resistance of the $Sm_{0.025}Sr_{0.975}MnO_3$ sample at room temperature .

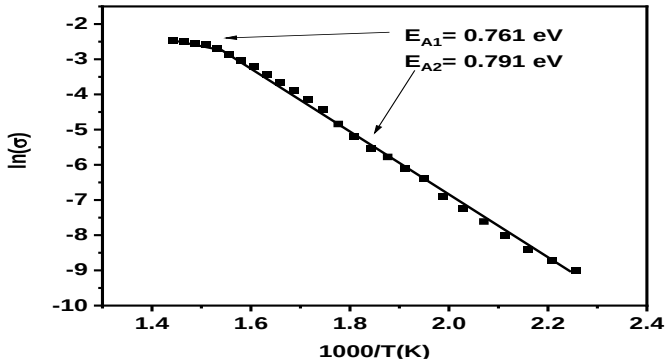

Figure 5: The relation between ln(σ) and 1000/T for fitting and obtaining the activation energy of $Sm_{0.025}Sr_{0.975}MnO_3$ sample.

When the relation between σ and T fitted; namely; ln(V) vs 1000/T, the activation energy, E_A, is obtained as illustrated in Fig. 5. It is understood that the temperature dependence of resistant is divided into two ranges; the longer range from 450K to 650 K and the second rang to the end of the temperature interval. So that, the sample has two activation energy values, E_{A2}=0.791 eV and E_{A1}=0.761 eV as illustrated in Fig. 5.

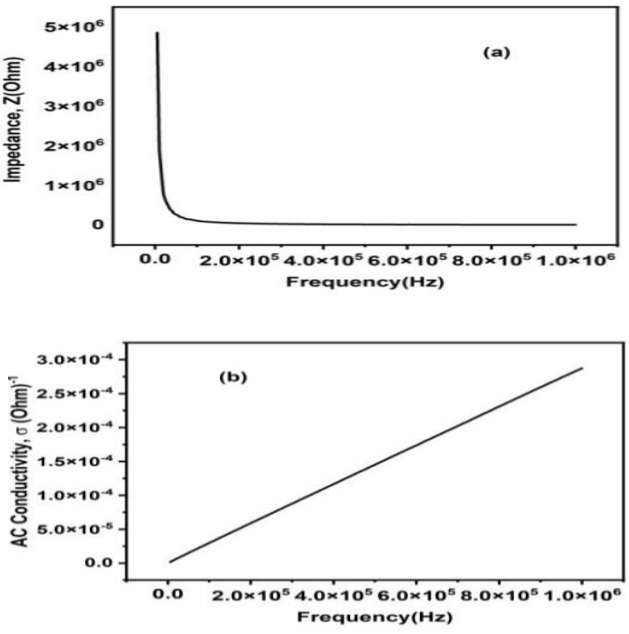

Figure 6: (a) The impedance, Z(Ω), and (b) the AC conductivity, σ(Ω.m)$^{-1}$, as functions of the AC current frequency, F(Hz), of $Sm_{0.025}Sr_{0.975}MnO_3$ sample.

3.3. Dielectric Properties

The dielectric properties study is very important in order to reveal the axial applications those may be make our compound used in industry or in scientific devices. In this section, the AC impedance, Z(Ω), AC conductivity, $\sigma(\Omega.m)^{-1}$, relative permitivity, ε, and the tangent loss factor, tan(δ), are investigated of the $Sm_{0.025}Sr_{0.975}MnO_3$ sample.

It is noticed in Fig (6a) that the impedance, Z(Ω), promptly decreases at low frequency reaching very low value, then, it does not change along the end of the frequency range. The reduction in Z(Ω) is because the resistance of the semiconductor materials has negative temperature coefficient [29, 30]. Iimpedance behavior of the sample makes it a candidate for possible use as an insulating material in the manufacture of capacitors. Regarding to the AC conductivity, $\sigma(\Omega.m)^{-1}$, it increases linearly through the whole range of the applied frequency, see Fig. (6b). It is illustrated that the AC conductivity has no DC component where it depends on the applied AC current frequency only. Through the high region of the frequency, the changes of σ_{AC} can obey to F^n relationship where n is a parameter subject to the temperature.

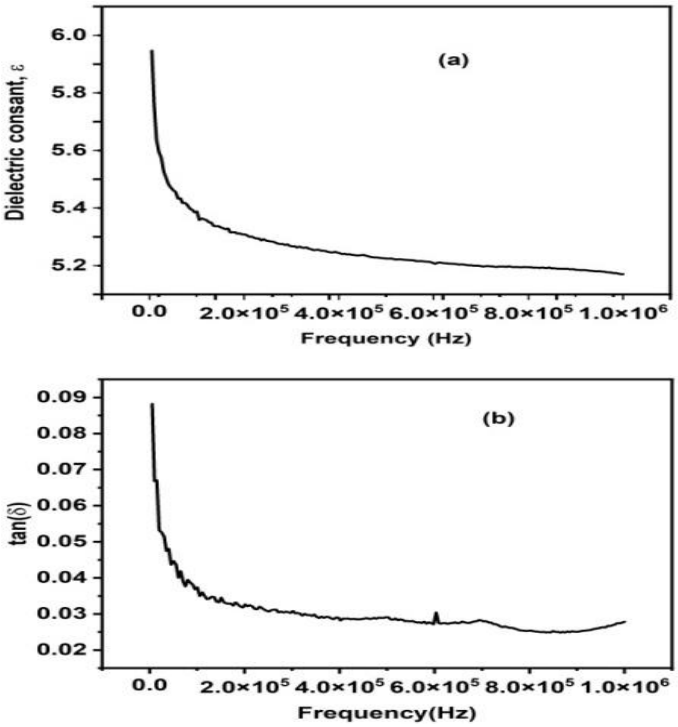

Figure 7: Dielectric constant ε, (a) and the dielectric loss factor, tan(δ) (b) as functions of AC current frequency, F(Hz), of $Sm_{0.025}Sr_{0.975}MnO_3$ sample.

The dielectric constant of $Sm_{0.025}Sr_{0.975}MnO_3$ sample which is shown in Fig. (7a) obeys the following equation [31]:

$$\varepsilon_r = \varepsilon = \frac{\varepsilon_m}{\varepsilon_0} = \varepsilon' - i\varepsilon'' \quad (4)$$

where $\boldsymbol{\varepsilon_r = \varepsilon}$ is the relative permittivity or the dielectric constant, $\boldsymbol{\varepsilon_m}$ is the the material permittivity, $\boldsymbol{\varepsilon'}$ is the real component and $\boldsymbol{\varepsilon''}$ is the imaginary component of the relative permittivity respectively. It is noticed that, ε reduces exponentially with increase of F(Hz) particularly along the low frequency range, then, tends to very low values at high frequency. The rotation direction at the boundaries might shed light on why the dielectric constant is relatively low at higher frequencies, as polarization is influenced by space charge effects. [32]. When an external electric field is applied, it can induce a dipole moment at the $Sm_{0.025}Sr_{0.975}MnO_3$ grain boundary interfaces. This effect allows atoms or ions to align with the AC electric field, leading to polarization in the direction of the rotation. [33].

Dielectric materials dissipate energy through the generation of absorption current. The following equation is used to calculate the tangent of the dielectric loss angle, tan(δ:

$$\tan(\delta) = \varepsilon''/\varepsilon' \quad (5)$$

tan(δ), which is shown in Fig. (7b), has exactly the same behavior as the relative dielectric constant behavior but it differs in values. The alignment of space charge carriers in a dielectric requires a finite amount of time for them to orient their axes parallel to an alternating field. As the frequency of the field reversal increases, there comes a point where the space charge carriers can no longer keep pace with the applied field. Consequently, their direction of alignment lags behind the applied field, leading to a decrease in the dielectric constant of the material [34].

4. Summary and Conclusions

In this work, the compound $Sm_xSr_{1-x}MnO_3$ (where x=0.025) was synthesized by the solid state reaction with annealing at 650ºC for 8 hours. The structure, morphological, electrical and dielectric properties of the compound $Sr_xSm_{1-x}MnO_3$were investigated. The most outstanding results obtained from this work are as following:

- X-rays diffraction results showed that the sample has monoclinic structure with a $Sm_{0.025}Sr_{0.975}MnO_3$ phase.
- SEM results showed plate-like perovskite grains which were clustered together in 150 nm average grains size.
- The electrical which measured by surface-surface contact showed a semiconductor behavior with increasing the ambient temperature. The sample had two activation energies; 0.791 eV and 0.761 eV.
- The impedance, Z(Ω), AC conductivity, $\sigma(\Omega.m)^{-1}$, dielectric constant, ε, and the dielectric loss factor, tan(δ), were investigated of the $Sm_{0.025}Sr_{0.975}MnO_3$ sample. The decrease in sample impedance makes it used as a dielectric material in the capacitors industry.
- The AC conductivity had no DC component where it depended on the applied AC current frequency only. The decrease of dielectric constant of the compound was interpreted to the lag of space charge carriers behind the applied AC field.

CRediT authorship contribution statement:

Conceptualization, H. M. Ali and Mahrous R. Ahmed; methodology, Mahrous R. Ahmed and Amira Etman; formal

analysis, M. M. Ibrahim; investigation, A. M. Abdel hakeem; resources, H. M. Ali; data curation, Amira Etman; writing-original draft preparation, Mahrous R. Ahmed; writing-review and editing, Mahrous R. Ahmed.; visualization, H. M. Ali; supervision, H. M. Ali; project administration, H. M. Ali; All authors have read and agreed to the published version of the manuscript."

Data availability statement

The data used to support the findings of this study are available from the corresponding author upon request.

Declaration of competing interest

The authors declare that they have no known competing financial interests or personal relationships that could have appeared to influence the work reported in this paper.

References

[1] M. B. Salamon and M. Jaime, *Rev. Mod. Phys.*, 73 (2001) 583.
[2] A. M. Ahmed, M. R Ahmed and S. A. Ahmed, *J. Electromagnetic Analysis & Applications*, 3 (2011) 27-32.
[3] I. A. Abdel-Latif, *JOURNAL OF PHYSICS*, 1 (2012) 15-31.
[4] C. N. R. Rao and B. Raveau, Colossal Magnetoresistance, Charge Ordering and Related Properties of manganese oxides, 1st Ed. World Scientific, New Delhi 1998.
[5] Y.Tokura, Y.Tomioka, *Journal of Magnetism and Magnetic Materials*, 200 (1999) 1-23.
[6] R. von Helmolt, J. Wecker, B. Holzapfel, L. Schultz and K. Samwer, *Physical Review Letters*, 71 (1993). 2331–2333.
[7] S. Jin, T. H. Tiefel, M. McCormack, R. A. Fastnacht, R. Ramesh and L. H. Chen, *Science*, 264 (1994) 413–5.
[8] M. Fiebig, Th. Lottermoser, D. Frohlich, A. V. Goltsev and R. V. Pisarev, *Nature*, 419 (2002) 818.
[9] A. I. Kurbakov, I. A. Abdel-Latif , M. R. Ahmed, H. U. Habermeier, A. Al-Hajry, A. L. Malyshev, V. A. Ulyanov, Th. M. El-Sherbini, *Eur. Phys. J. Plus*, 137 (2022) 658.
[10] S. V. Ovsyannikov, M. Bykov, E. Bykova, K. Glazyrin, R.S. Manna, A.A. Tsirlin and L. S. Dubrovinsky, *Nat. Commun*., 9 (2018) 4142.
[11] M. R. Ahmed, *Journal of Magnetism and Magnetic Materials*, 504 (2020) 166628.
[12] M. R. Ahmed and G. A. Gehring, *J. Phys. A: Math. Gen*., 38 (2005) 4047–4067.
[13] M. R. Ahmed and G. A. Gehring, *physical review B*, 74 (2006) 014420.
[14] M. R. Ahmed, A. M. Ahmed, A. K. Diab and S. M. Abo-elhasan, *Sohag J. Sci.*, 7 (2022) 9- 14.
[15] V. Skumryev, F. Ott, J. M. D. Coey, *J. Phys. Condens. Matter*, 11 (1999) 401-406.
[16] P. Saxena and A. Mishra, *Journal of Solid State Physics*, 301 (2021) 122364.
[17] A. I. Kurbakov, C. Martin, A. Maignan, *Journal of Magnetism and Magnetic Materials*, 321 (2009) 2601–2606.
[18] I. D. Luzyanin, V. A. Ryzhov, D. Yu. Chernyshov, A. I. Kurbakov, V. A. Trounov, A. V. Lazuta, V. P. Khavronin, I. I. Larionov and S. M. Dunaevsky, *Phys. Rev. B*, 64 (2001) 094432.
[19] J. M. De Teresa, M. R. Ibarra, P. Algarabel, L. Morellon, B. Garcı´a-Landa, C. Marquina, C. Ritter, A. Maignan, C. Martin, B. Raveau, A. Kurbakov and V. Trounov, *Phys. Rev. B*, 65 (2002) R100403.
[20] A. I. Kurbakov, A. V. Lazuta and V. A. Ryzhov, *Journal of Physics: Conference Series*, 200 (2010) 012099.
[21] A. I. Kurbakov, V. A. Trounov, A. M. Balagurov, V. Yu. Pomyakushin, D. V. Sheptyakov, O. Yu. Gorbenko and A. R. Kaul, *Phys. Solid State*, 46 (2004) 1704.
[22] A. I. Kurbakov, A. V. Lazuta, V. A. Ryzhov, V. A. Trounov, I. I. Larionov, C. Martin, A. Maignan, M. Hervieu, *Phys. Rev. B*, 72 (2005) 184432.
[23] A. I. Kurbakov, C. Martin and A. Maignan, *J. Phys.: Condens. Matter*, 20 (2008) 104233.
[24] M. R. Ahmed, H. M. Ali, M. F. Hasaneen, Amira Etman and A. M. Abdel hakeem, *Inf. Sci. Lett.*, 11 (2022) 457- 463.
[25] A. E. Hannora and F. F. Hanna, *Journal of Materials Science: Materials in Electronics*, 30 (2019) 12456–12464.
[26] A. I. Kurbakov, C. Martin and A. Maignan, *Journal of Magnetism and Magnetic Materials*, 321 (2009) 2601–2606.
[27] C. Saravanana, R. Thiyagarajan, P. V. Kanjariyad, P. Sivaprakasha, J. A. Bhalodiad and S. Arumugam, *Journal of Magnetism and Magnetic Materials*, 476 (2019) 35-39.
[28] P. V. Kanjariya, G. D. Jadav, C. Saravanan, L. Govindaraj, S. Arumugam and J. A. Bhalodia, *J. Mater. Sci.: Mater. Electron.*, 29 (2018) 8107.
[29] N. Kumari, V. Kumar and S. K. Singh, *RSC Adv.*, 5 (2015) 37925–37934.
[30] L. S. Lobo and A. R. Kumar, *J. Mater. Sci. Mater. Electron.*, 27 (2016) 7398–7406.
[31] M. R. Ahmed, E. Kh. Shokr, I. A. Abdel-Latif, Ibrahim Y. Khaled, E. M. M. Ibrahim and Sara A. Mohamed, *the European Physical Journal B*, 97 (2024) 114.
[32] S. Singh, P. Dey, J. N. Roy and S. K. Mandal, *Appl. Phys. Lett.*, 105 (2014) 092903.
[33] Ç. Oruç and A. Altındal, *Ceram. Int.*, 43 (2017) 10708–10714.
[34] A. M. Shaikh, S. S. Bellad and B. K. Chougule, *Journal of Magnetism and Magnetic Materials*, 195 (1999) 384.